Adaptive observer-based sliding mode control with time-varying learning using Riccati gain synthesis for robotic manipulators

Hoang Duc Long*

Institute of Control Engineering, Le Quy Don Technical University, 236 Hoang Quoc Viet, Hanoi, Vietnam.
*Corresponding author: longhd@lqdtu.edu.vn
Received 5 Jul. 2025; Revised 15 Sep. 2025; Accepted 10 Nov. 2025; Published 28 Nov. 2025.
DOI: https://doi.org/10.54939/1859-1043.j.mst.107.2025.13-23

ABSTRACT

This paper presents an adaptive observer-based sliding mode control (AOSMC) framework integrated with time-varying learning rates and Riccati gain synthesis (RGS) for high-precision trajectory tracking of robotic manipulators under dynamic uncertainties and external disturbances. Conventional sliding mode control methods, while robust, often suffer from high chattering and require precise knowledge of system bounds. To address these limitations, the proposed AOSMC-RGS architecture combines a nonlinear disturbance observer with Riccati-based adaptive gain tuning, enabling real-time disturbance estimation and dynamic gain adjustment based on tracking errors. A rigorous Lyapunov stability analysis ensures boundedness and convergence of system states. Simulation studies on a 2-DOF robotic manipulator demonstrate significant improvements in tracking accuracy, disturbance rejection, and control smoothness compared to PID, SMC, ASMC, Fuzzy-ASMC, and RBF-ASMC controllers. The proposed approach achieves reduced overshoot, faster settling time, and lower control effort while maintaining robustness, making it a promising candidate for real-time robotic and mechatronic system applications.

Keywords: Adaptive control; Sliding mode control; Riccati equation; Disturbance observer; Robotic manipulators; Time-varying learning rate.

1. INTRODUCTION

Robust control of robotic manipulators is challenging due to nonlinear dynamics, uncertainties, and disturbances [1-5]. While Sliding Mode Control (SMC) ensures robustness, it suffers from high chattering and requires large switching gains. Adaptive SMC (ASMC) has been developed to address these issues [1], including extensions such as integral ASMC with time-delay estimation [2] and approaches for unknown friction and control direction [3]. However, these methods may still face limitations in adaptation speed, complexity, and practical implementation. To enhance adaptability, gain adjustment strategies using fuzzy logic (Fuzzy-ASMC) [4] and neural networks (RBF-ASMC) [5] have been proposed, but they often rely on heuristic tuning or require persistent excitation, making them less systematic. To overcome these drawbacks, this work introduces the Adaptive Observer-Based Sliding Mode Control with Riccati Gain Synthesis (AOSMC-RGS), designed to achieve improved tracking accuracy, faster disturbance rejection, and reduced chattering compared with PID, SMC, ASMC, Fuzzy-ASMC, and RBF-ASMC controllers.

The remainder of this paper is organized as follows: Section 2 introduces the mathematical model of the robotic manipulator. Section 3 presents the design of the nonlinear state and disturbance observers, the adaptive sliding mode controller, and explains the Riccati gain adaptation mechanism. Section 4 provides the stability analysis. Section 5 details the simulation setup and presents the results and discussion. Section 6 concludes the paper and outlines potential future research directions.

2. MATHEMATICAL MODEL OF THE SYSTEM

2.1. Overview of the 2-DOF robotic manipulator

Two-degree-of-freedom (2-DOF) robotic manipulators have many applications in practical systems [6, 7]. The dynamic modeling of a 2-DOF robotic manipulator is shown in figure 1. It consists of two rotary joints, typically actuated independently, that allow the end-effector to move within a plane. This simplified system retains key nonlinear dynamic properties of high-DOF manipulators while enabling compact analysis and control design. Each joint angle $q_i \in \mathbb{R}$ is measured with respect to a fixed base frame, and the system's dynamics are governed by the laws of rigid-body motion.

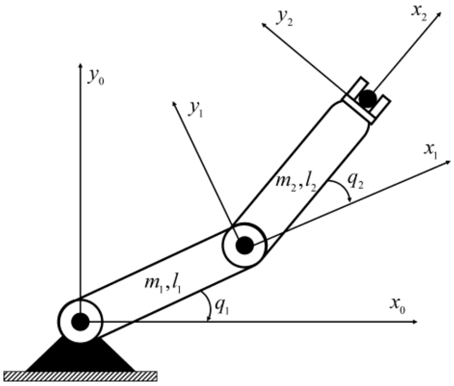

Figure 1. *The 2-DoF robot manipulator.*

2.2. Dynamic equations of motion

The general form of the Euler-Lagrange dynamic model of a 2-DOF robotic manipulator is given by [7]:

$$M(q)\ddot{q} + C(q,\dot{q})\dot{q} + G(q) + D(t) = \tau \tag{1}$$

where $q = [q_1, q_2]^T \in \mathbb{R}^2$ is the joint position vector, $\dot{q}, \ddot{q} \in \mathbb{R}^2$ are the velocity and acceleration vectors, $M(q) \in \mathbb{R}^{2\times 2}$ is the symmetric positive definite inertia matrix, $C(q,\dot{q}) \in \mathbb{R}^{2\times 2}$ is the Coriolis and centrifugal matrix, $G(q) \in \mathbb{R}^2$ is the gravity vector, $\tau = [\tau_1, \tau_2]^T \in \mathbb{R}^2$ is the control input, $D(t) \in \mathbb{R}^2$ represents unknown external disturbances and unmodeled dynamics. The model assumes rigid links, negligible friction, and full state measurability.

Given link masses m_1, m_2, lengths l_1, l_2, and gravity g, the matrices are:

- Inertia matrix $M(q)$:

$$M(q) = \begin{bmatrix} m_1 l_1^2 + m_2\left(l_1^2 + l_2^2 + 2l_1 l_2 \cos q_2\right) & m_2\left(l_2^2 + l_1 l_2 \cos q_2\right) \\ m_2\left(l_2^2 + l_1 l_2 \cos q_2\right) & m_2 l_2^2 \end{bmatrix} \tag{2}$$

- Coriolis and centrifugal matrix $C(q,\dot{q})$:

$$C(q,\dot{q}) = \begin{bmatrix} -m_2 l_1 l_2 \sin q_2 \dot{q}_2 & m_2\left(l_2^2 + l_1 l_2 \cos q_2\right) \\ m_2 l_1 l_2 \sin q_2 \dot{q}_1 & 0 \end{bmatrix} \tag{3}$$

- Gravity vector $G(q)$:

$$G(q) = \begin{bmatrix} (m_1 + m_2) g l_1 \sin q_1 + m_2 g l_2 \sin(q_1 + q_2) \\ m_2 g l_2 \sin(q_1 + q_2) \end{bmatrix} \tag{4}$$

2.3. Assumptions

- **Assumption 1 (Bounded initial states)**. There exists a bounded set

$$\chi_0 = \left\{ \left(q(0), \dot{q}(0) \right) \in \mathbb{R}^n \ \mid \ \|q(0)\| \le q_{\max}, \ \|\dot{q}(0)\| \le \dot{q}_{\max} \right\} \tag{5}$$

such that the initial states of the system satisfy

$$\left(q(0), \dot{q}(0) \right) \in \chi_0 \tag{6}$$

where $q_{\max} > 0$ and $\dot{q}_{\max} > 0$ are known finite constants.

- **Assumption 2**. The mass matrix $M(q)$ is symmetric and uniformly positive definite:

$$\exists \alpha_1, \alpha_2 > 0: \ \alpha_1 I \le M(q) \le \alpha_2 I, \quad \forall q \in \mathbb{R}^2 \tag{7}$$

- **Assumption 3**. The Coriolis matrix satisfies $\dot{M}(q) - 2C(q, \dot{q})$ is skew-symmetric.
- **Assumption 4**. The disturbance $d(t) \in \mathbb{R}^2$ is bounded and differentiable:

$$\|D(t)\| \le D_{\max}, \quad \|\dot{D}(t)\| \le L_D \tag{8}$$

The control objective is to design a robust control law τ that ensures asymptotic trajectory tracking despite uncertainties and disturbances.

3. ADAPTIVE OBSERVER-BASED SLIDING MODE CONTROL WITH RICCATI GAIN SYNTHESIS

In this section, we propose an AOSMC-RGS, which incorporates an adaptive gain mechanism and a disturbance observer, and we provide a proof of finite-time convergence.

3.1. Nonlinear state observer

Assume the state variables $x_1 = q = [q_1, q_2]^T$ are measurable and $x_2 = \dot{q} = [\dot{q}_1, \dot{q}_2]^T$ are unmeasurable. The nonlinear state observer is designed based on the Luenberger observer structure adapted for nonlinear systems, enabling estimation of unmeasured states in robotic manipulators. The outputs of the nonlinear observer are $\hat{x}_1 = \hat{q} = [\hat{q}_1, \hat{q}_2]^T \in \mathbb{R}^2$ and $\hat{x}_2 = \dot{\hat{q}} = \left[\dot{\hat{q}}_1, \dot{\hat{q}}_2 \right]^T$.

Theorem 1.

Consider the 2-DOF robotic manipulator with dynamics:

$$M(x_1)\dot{x}_2 + C(x_1, x_2)x_2 + G(x_1) = \tau \tag{9}$$

and the nonlinear observer:

$$\begin{cases} \dot{\hat{x}}_1 = \hat{x}_2 + L_1(x_1 - \hat{x}_1) \\ \dot{\hat{x}}_2 = M^{-1}(\hat{x}_1)\left(\tau - C(\hat{x}_1, \hat{x}_2)\hat{x}_2 - G(\hat{x}_1)\right) + L_2(x_1 - \hat{x}_1) \end{cases} \tag{10}$$

where $L_1, L_2 \in \mathbb{R}^{2\times 2}$ are positive definite matrices.

Then, the observer error $\tilde{x}_1 = x_1 - \hat{x}_1$, $\tilde{x}_2 = x_2 - \hat{x}_2$ converges exponentially to zero.

Proof. Define the observation errors:

$$\tilde{x}_1 = x_1 - \hat{x}_1, \ \tilde{x}_2 = x_2 - \hat{x}_2 \tag{11}$$

Then, we have:

$$\dot{\tilde{x}}_1 = \dot{x}_1 - \dot{\hat{x}}_1 = x_2 - \hat{x}_2 - L_1\tilde{x}_1 = \tilde{x}_2 - L_1\tilde{x}_1 \tag{12}$$

To derive the error dynamics for $\tilde{x}_2$, we write:

$$\dot{\tilde{x}}_2 = \dot{x}_2 - \dot{\hat{x}}_2 = M^{-1}(x_1)\big(\tau - C(x_1,x_2)x_2 - G(x_1)\big) \\ - M^{-1}(\hat{x}_1)\big(\tau - C(\hat{x}_1,\hat{x}_2)\hat{x}_2 - G(\hat{x}_1)\big) - L_2\tilde{x}_1 \quad (13)$$

Let's define the mismatch:

$$\Delta(x_1,x_2,\dot{x}_1,\dot{x}_2) = M^{-1}(x_1)\big(\tau - C(x_1,x_2)x_2 - G(x_1)\big) \\ - M^{-1}(\hat{x}_1)\big(\tau - C(\hat{x}_1,\hat{x}_2)\hat{x}_2 - G(\hat{x}_1)\big) \quad (14)$$

Under smoothness (Lipschitz continuity) assumptions, there exists a constant

$$\|\Delta\| \le \rho\big(\|\tilde{x}_1\| + \|\tilde{x}_2\|\big) \quad (15)$$

Therefore:

$$\dot{\tilde{x}}_2 = -L_2\tilde{x}_1 + \Delta(x_1,x_2,\dot{x}_1,\dot{x}_2) \quad (16)$$

Let us choose the Lyapunov function:

$$V_1 = \frac{1}{2}\tilde{x}_1^T P_1\tilde{x}_1 + \frac{1}{2}\tilde{x}_2^T P_2\tilde{x}_2 \quad (17)$$

where $P_1, P_2 > 0$ are symmetric positive definite matrices.

Compute its derivative:

$$\dot{V}_1 = \tilde{x}_1^T P_1\dot{\tilde{x}}_1 + \tilde{x}_2^T P_2\dot{\tilde{x}}_2 \quad (18)$$

Substitute:

$$\dot{\tilde{x}}_1 = \tilde{x}_2 - L_1\tilde{x}_1, \quad \dot{\tilde{x}}_2 = -L_2\tilde{x}_1 + \Delta(x_1,x_2,\dot{x}_1,\dot{x}_2) \quad (19)$$

Then:

$$\dot{V}_1 = -\tilde{x}_1^T P_1 L_1\tilde{x}_1 - \tilde{x}_2^T P_2 L_2\tilde{x}_1 + \tilde{x}_1^T P_1\tilde{x}_2 + \tilde{x}_2^T P_2\Delta \quad (20)$$

Using Young's inequality: $\tilde{x}_1^T P_1\tilde{x}_2 \le \frac{1}{2}\tilde{x}_1^T P_1^2\tilde{x}_1 + \frac{1}{2}\tilde{x}_2^T\tilde{x}_2$ and $\tilde{x}_2^T P_2\Delta \le \frac{1}{2}\tilde{x}_2^T P_2^2\tilde{x}_2 + \frac{1}{2}\Delta^T\Delta$

Thus:

$$\dot{V}_1 \le -\lambda_1\|\tilde{x}_1\|^2 - \lambda_2\|\tilde{x}_1\|\|\tilde{x}_2\| + c_1\|\tilde{x}_1\|^2 + c_2\|\tilde{x}_2\|^2 \quad (21)$$

Choosing L_1, L_2 sufficiently large ensures:

$$\dot{V}_1 \le -\alpha V_1 \quad (22)$$

for some $\alpha > 0$, which implies exponential convergence of the observation error.

The observer error dynamics are globally exponentially stable. That is,

$$\|\tilde{x}_1\| + \|\tilde{x}_2\| \le Ce^{-\alpha t} \quad (23)$$

for constants $C > 0,\ \alpha > 0.$

3.2. Disturbance observer

A high-gain disturbance observer structure is employed for real-time disturbance estimation to enhance robustness without requiring full model knowledge, as shown below.

$$\hat{D}(t) = \int_0^t \eta(\tau)d\tau, \quad \dot{\eta} = -l\big(\eta - D(t)\big), \quad l \gg 1 \quad (24)$$

This ensures $\hat{D}(t) \to D(t)$ exponentially fast under Assumption 4.

3.3. Adaptive sliding mode control

Using the manipulator dynamics (1) and state observer (8), let the tracking error be defined as:

$$\hat{e}(t)=\hat{x}_1(t)-q_d(t),\quad \dot{\hat{e}}(t)=\hat{x}_2(t)-\dot{q}_d(t) \tag{25}$$

where $q_d=\left[q_{1d},q_{2d}\right]^T\in\mathbb{R}^2$ is the vector of desired trajectories and $\dot{q}_d$ is its derivative.

The sliding surface is defined as:

$$s(t)=\hat{e}_2(t)+\Lambda\hat{e}_1(t) \tag{26}$$

where $\Lambda\in\mathbb{R}^{2\times 2}$, $\Lambda>0$.

The adaptive sliding mode control law is designed as below:

$$\tau(t)=\tau_{eq}(t)+\tau_{sw}(t) \tag{27}$$

with the equivalent control $\tau_{eq}(t)$ is

$$\tau_{eq}(t)=M(\hat{x}_1)\ddot{q}_d+C(\hat{x}_1,\hat{x}_2)\hat{x}_2+G(\hat{x}_1)+\hat{D}(t) \tag{28}$$

and the switching control $\tau_{sw}(t)$ is

$$\tau_{sw}(t)=-K(t)\mathrm{sat}\left(\frac{s}{\phi}\right) \tag{29}$$

where $K(t)$ is an adaptive gain matrix (positive-definite), $\mathrm{sat}(\cdot)$ is the saturation function (continuous approximation of sign), $\phi>0$ is the boundary layer width.

3.4. Adaptive gain update via Riccati-type equation

The derivative of the sliding surface is:

$$\begin{aligned}\dot{s}&=M^{-1}(\hat{x}_1)\left(\tau-C(\hat{x}_1,\hat{x}_2)\hat{x}_2-G(\hat{x}_1)-D\right)-\ddot{q}_d+\Lambda\hat{e}_2\\&=-M^{-1}(\hat{x}_1)K\mathrm{sat}\left(\frac{s}{\phi}\right)-M^{-1}(\hat{x}_1)\left(D-\hat{D}\right)+\Lambda\hat{e}_2\end{aligned} \tag{30}$$

Neglecting the disturbance estimation error and replacing $\mathrm{sat}\left(\frac{s}{\phi}\right)$ by s in boundary layers:

$$\dot{s}\approx A(\hat{x}_1,\hat{x}_2)s+B(\hat{x}_1)u \tag{31}$$

where $A(\hat{x}_1,\hat{x}_2)=-M^{-1}(\hat{x}_1)K$, $B(\hat{x}_1)=\Lambda$, $u=\hat{e}_2$.

Define the objective function:

$$J(t)=\int_0^{\infty}\left(s^TQs+\hat{e}_2^TR\hat{e}_2\right)dt \tag{32}$$

where $Q\in\mathbb{R}^{2\times 2}$ positive-definite matrix that penalizes error, $R\in\mathbb{R}^{2\times 2}$ penalizes control effort.

We define the adaptive gain as:

$$\dot{K}(t)=-P(t)s(t)\mathrm{sign}\left(s(t)\right) \tag{33}$$

where the matrix $P(t)\in\mathbb{R}^{2\times 2}$ is found by solving the Riccati equation:

$$\dot{P}=A^T(\hat{x}_1,\hat{x}_2)P+PA(\hat{x}_1,\hat{x}_2)-PB(\hat{x}_1)R^{-1}B^T(\hat{x}_1)P+Q \tag{34}$$

The solution of the Riccati equation guarantees $J(t)\to\min$ so that $s(t)$ and $\hat{e}_2(t)\to\min$.

The block diagram of the proposed algorithm is demonstrated in figure 2 below.

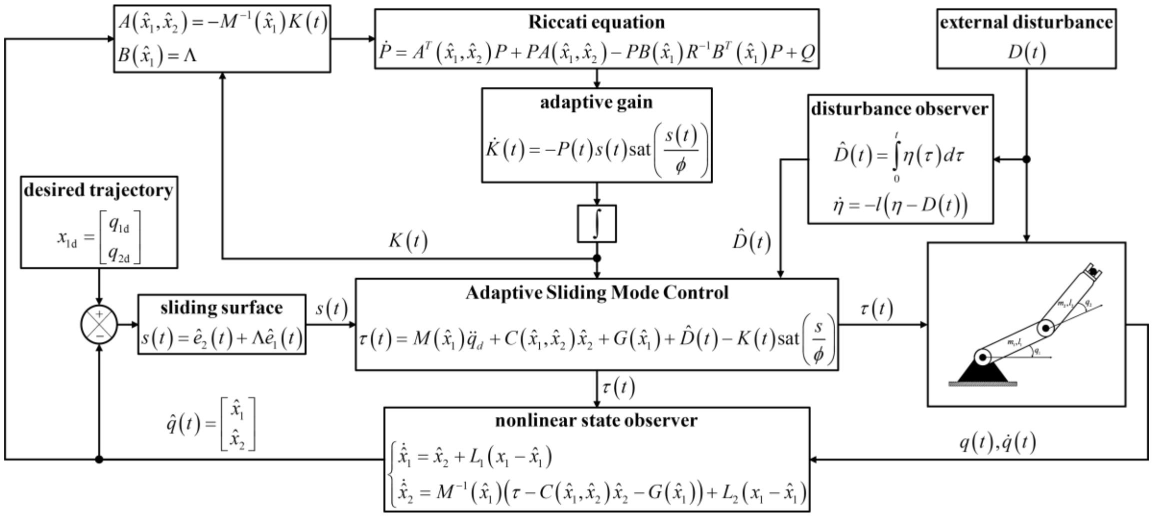

Figure 2. *The block diagram of AOSMC-RGS.*

4. STABILITY AND FINITE-TIME CONVERGENCE

Using the outputs of the state observer, the equation of the 2-DOF robotic manipulator is rewritten as:

$$M(\hat{x}_1)\dot{\hat{x}}_2 + C(\hat{x}_1,\hat{x}_2)\hat{x}_2 + G(\hat{x}_1) + D(t) = \tau \tag{35}$$

Theorem 2.

Under Assumptions 1-4, the AOSMC-RGS control law ensures: $\lim_{t\to\infty}\|\hat{e}_1(t)\| = 0$*; Finite-time convergence of the tracking error; Boundedness of all closed-loop signals.*

Proof. Define Composite Lyapunov Function

$$V_2 = \frac{1}{2}s^T M(\hat{x}_1)s + \frac{1}{2}\text{tr}(P) \tag{36}$$

The derivative of

$$\begin{aligned}\dot{V}_2 &= s^T M(\hat{x}_1)\dot{s} + \frac{1}{2}s^T\dot{M}(\hat{x}_1)s + \frac{1}{2}\text{tr}(\dot{P}) \\ &= -s^T K\text{sat}\left(\frac{s}{\phi}\right) - s^T(D - \hat{D}) + s^T M(\hat{x}_1)(\Lambda\hat{e}_2) + \frac{1}{2}s^T\dot{M}(\hat{x}_1)s + \frac{1}{2}\text{tr}(\dot{P})\end{aligned} \tag{37}$$

Use $\dot{P}$ from the Riccati equation:

$$\text{tr}(\dot{P}) = \text{tr}(A^T P + PA) - \text{tr}(PBR^{-1}B^T P) + \text{tr}(Q) \tag{38}$$

If $\|D - \hat{D}\| \le \delta$, then:

$$\dot{V}_2 \le -\lambda_{\min}(K)\|s\| + \|s\|\delta + \text{bounded term} \tag{39}$$

Choose $K(t)$ such that $\lambda_{\min}(K) > \delta$. Then:

$$\dot{V}_2 \le -c\|s\| \tag{40}$$

where $c = \lambda_{\min}(K) - \delta > 0$, therefore:

$$\lim_{t\to\infty}s(t) = 0 \Rightarrow \lim_{t\to\infty}\hat{e}_1(t) = 0 \tag{41}$$

Under the designed AOSMC-RGS controller, the sliding surface $s(t)$ converges to zero in finite time, with the settling time bounded by:

$$T \le \frac{V_2(0)}{c\sigma} \tag{42}$$

where $V_2(0)$ is the initial value of the Lyapunov function, $c > 0$ is the positive convergence rate constant, $\sigma > 0$ is the desired precision.

5. SIMULATION RESULTS AND DISCUSSION

The parameters of a 2-DOF robotic manipulator are used for simulation: $m_1 = m_2 = 1(kg)$, $l_1 = l_2 = 1(m)$, $g = 9.81(m/s^2)$. The desired trajectories: $[q_{1d},\ q_{2d}]^T = [\sin 2t,\ 0.5\sin 3t]^T$. The parameters of AOSMC-RGS: $\Lambda_{SMC} = \text{diag}\{6, 6\}$, $\phi = 0.01$, $K(0) = \text{diag}\{5, 5\}$, $P(0) = \text{diag}\{10, 10\}$. The tracking error: $e_1 = \hat{x}_1 - q_d$, $e_2 = \dot{e} = \hat{x}_2 - \dot{q}_d$. The parameters of state observer: $L_1 = \text{diag}\{30, 30\}$, $L_2 = \text{diag}\{50, 50\}$. The initial values: $[q_1(0),\ q_2(0)]^T = [\pi,\ -\pi]^T$, $[\dot{q}_1(0),\ \dot{q}_2(0)]^T = [0,\ 0]^T$, $[\hat{q}_1(0),\ \hat{q}_2(0)]^T = [0,\ 0]^T$, $[\dot{\hat{q}}_1(0),\ \dot{\hat{q}}_2(0)]^T = [0,\ 0]^T$.

To show the effectiveness of the proposed algorithm, two scenarios are considered as below.

- **First scenario (FS)**: The desired trajectories: $q_d(t) = [\sin(2t), 0.5\sin(3t)]^T$; the initial positions: $q_0 = [\pi, -\pi]^T$; the external disturbances: $D(t) = [0.5\sin 3t, 0.4\cos 4t]^T$.

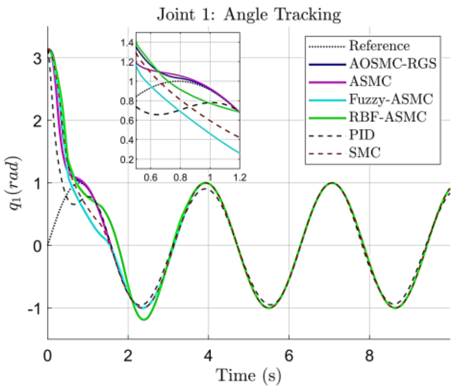

Figure 3. *Angle of joint 1 in FS.*

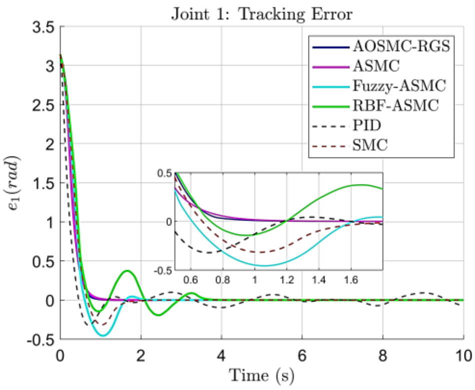

Figure 4. *Tracking error of joint 1 in FS.*

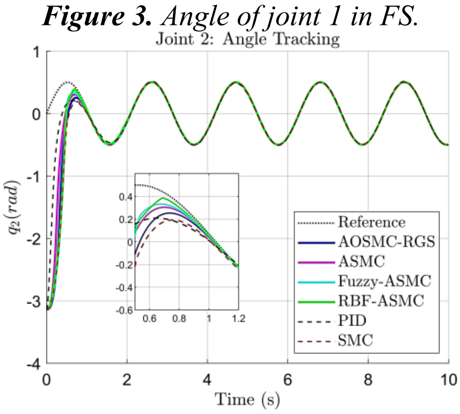

Figure 5. *Angle of joint 2 in FS.*

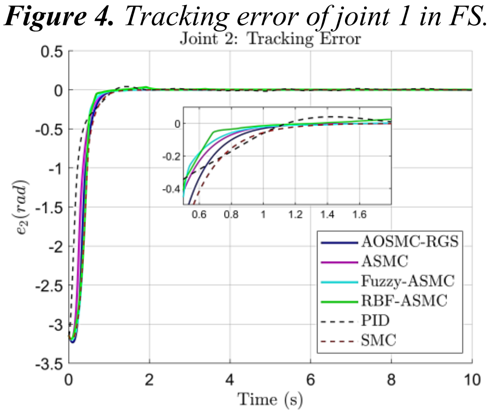

Figure 6. *Tracking error of joint 2 in FS.*

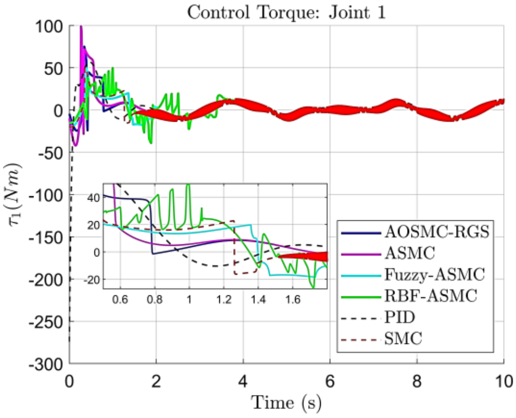

Figure 7. *Control law of joint 1 in FS.*

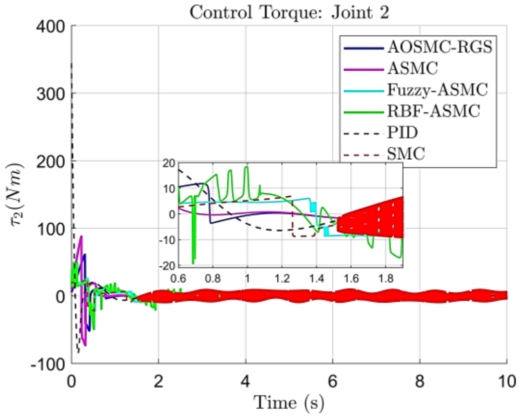

Figure 8. *Control law of joint 2 in FS.*

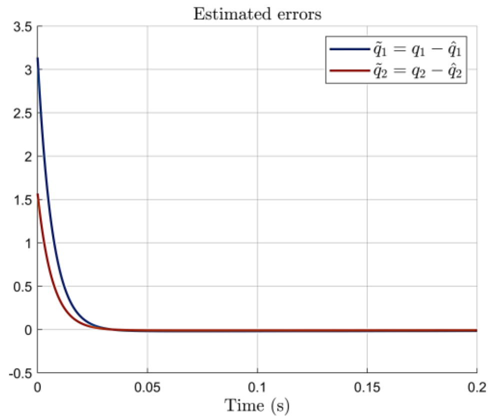

Figure 9. *Estimated errors of joints in FS.*

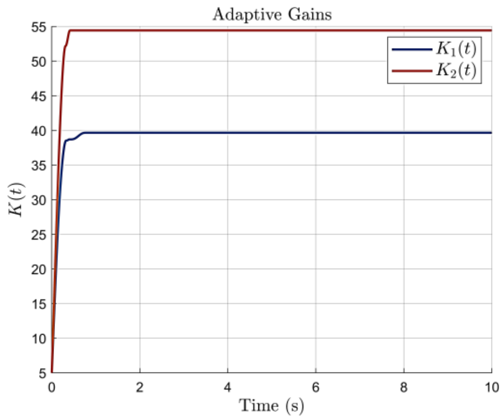

Figure 10. *Adaptive gains in FS.*

Root Mean Squared Error (RMSE) definition for joint j is given below.

$$RMSE_j = \sqrt{\frac{1}{N}\sum_{k=1}^{N}\left(e_j(k)\right)^2} = \sqrt{\frac{1}{N}\sum_{k=1}^{N}\left(q_j(k) - q_{dj}(k)\right)^2} \tag{43}$$

RMSE (q1, q2) for each controller in the first scenario:

	AOSMC-RGS	ASMC	Fuzzy-ASMC	RBF-ASMC	PID	SMC
RMSE(q1)	0.3538	0.4461	0.4869	0.5086	0.5847	0.4822
RMSE(q2)	0.3542	0.5019	0.5825	0.5747	0.5872	0.5683

- **Second scenario (SS)**:

The desired trajectories: $q_d(t) = \left[0.5a_1\left(\text{square}(\pi ft)+1\right), 0.5a_2\left(\text{square}(\pi ft)+1\right)\right]^T$;

The initial positions: $q_0 = [0, -1]^T$;

The external disturbances: $[d_1,\ d_2]^T = [0.5\cos 3t,\ 0.4\sin 4t]^T$.

RMSE (q1, q2) for each controller in the second scenario:

	AOSMC-RGS	ASMC	Fuzzy-ASMC	RBF-ASMC	PID	SMC
RMSE(q1)	0.3575	0.3723	0.4401	0.3837	0.5787	0.4613
RMSE(q2)	0.2234	0.2437	0.2267	0.2330	0.2517	0.2335

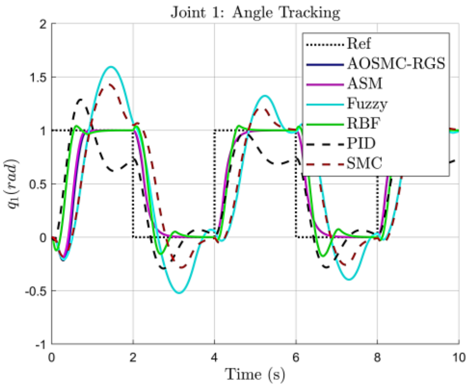

Figure 11. *Angle of joint 1 in SS.*

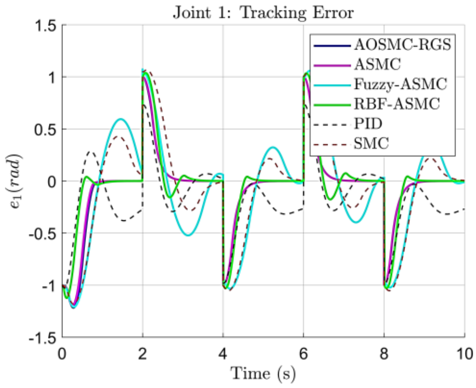

Figure 12. *Tracking error of joint 1 in SS.*

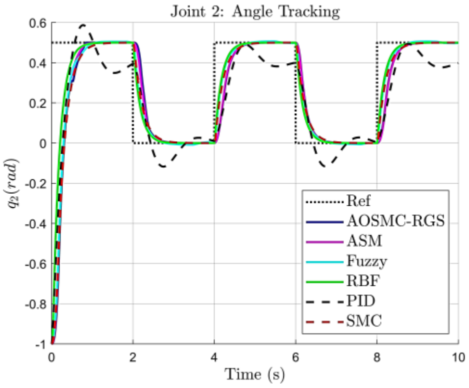

Figure 13. *Angle of joint 2 in SS.*

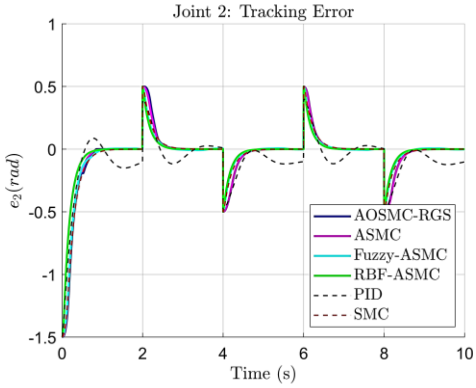

Figure 14. *Tracking error of joint 2 in SS.*

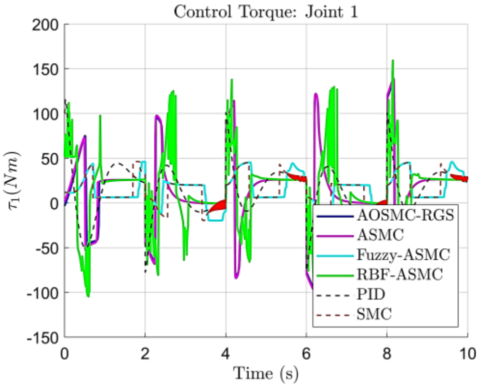

Figure 15. *Control law of joint 1 in SS.*

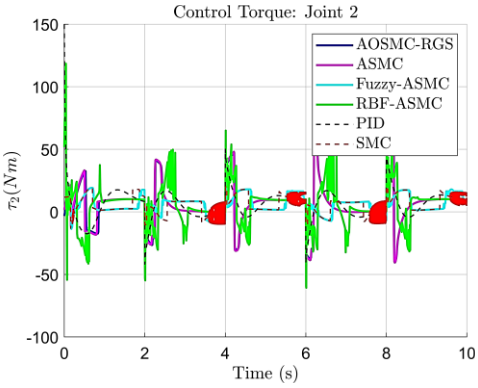

Figure 16. *Control law of joint 2 in SS.*

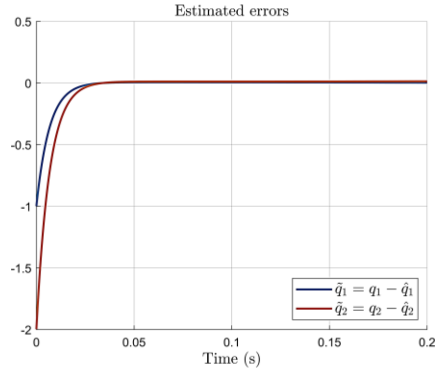

Figure 17. *Estimated error of Joint 1 in SS.*

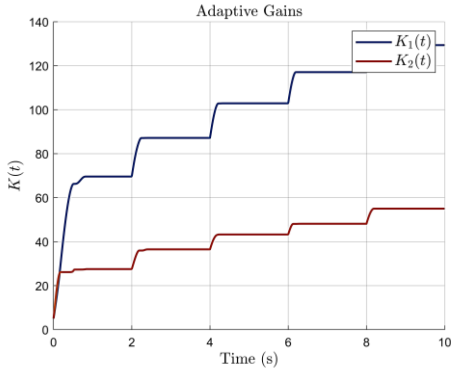

Figure 18. *Adaptive gains in SS.*

Conclusion of simulated results: Figures 3-6 and figures 11-14 illustrate the tracking performances of PID control, SMC, ASMC, Fuzzy-ASMC, RBF-ASMC, and the proposed AOSMC-RGS. The AOSMC-RGS controller demonstrates superior tracking with reduced overshoot, faster settling time, and lower steady-state error compared to the other algorithms. Figures 7-8 and figures 15-16 display the control inputs generated by the controllers. The AOSMC-RGS produces smaller control amplitudes than the other controllers while maintaining effective tracking performance and reducing the chattering effect. Figure 9 and figure 17 demonstrate the performance of the nonlinear state observer, which efficiently estimates the unmeasured states with minimal estimation errors. Figure 10 and figure 18 present the adaptive gain trajectories obtained via Riccati gain synthesis during the control process. These adaptive gains adjust dynamically in response to the system states, enabling the controller to balance convergence speed and control effort effectively while preserving robustness.

Overall, the simulation results confirm that the proposed AOSMC-RGS controller achieves high-precision trajectory tracking, improved disturbance rejection, and smoother control effort compared to conventional methods, validating its potential for real-time robotic applications.

6. CONCLUSIONS

This paper presented an Adaptive Observer-Based Sliding Mode Control with Riccati Gain Synthesis (AOSMC-RGS) for robotic manipulators under uncertainties and disturbances. By integrating disturbance observation, adaptive gain tuning, and a time-varying learning rate, the method achieves high tracking accuracy, reduced chattering, and improved robustness compared with PID, SMC, ASMC, Fuzzy-ASMC, and RBF-ASMC. Simulation results confirm that AOSMC-RGS offers smoother control effort, faster adaptation, and better disturbance rejection, making it a reliable solution for high-performance robotic applications.

Future work will focus on the real-time implementation of the AOSMC-RGS on physical robotic platforms in dynamic environments.

REFERENCES

[1]. Li, R., Yang, L., Chen, Y., and Lai, G., "*Adaptive Sliding Mode Control of Robot Manipulators with System Failures*," Mathematics, Vol. 10, No. 3, 339, (2022), doi: 10.3390/math10030339.

[2]. Lee, J., Chang, P. H., and Jin, M., "*Adaptive Integral Sliding Mode Control With Time-Delay Estimation for Robot Manipulators*," IEEE Transactions on Control Systems Technology, Vol. 25, No. 6, pp. 2056–2063, (2017), doi: 10.1109/TIE.2017.2698416.

[3]. S. H. Han *et al.*, "*Adaptive Sliding Mode Control for a Robotic Manipulator with Unknown Friction and Unknown Control Direction*," Applied Sciences, vol. 11, no. 9, (2021), doi: 10.3390/app11093919.

[4]. Phi, H. N., and Nguyen, D. H., "*Điều khiển trượt thích nghi mờ cho Robot 3 bậc tự do RPP*," Journal of Science & Technology - Hanoi University of Industry, Vol. 64, No. 5, pp. 36-43, 2022, doi: 10.57001/huih5804.81 (in Vietnamese).

[5]. Phan, D. H., and Le, N. D., "*Điều khiển thích nghi lực/vị trí cho robot tay máy sử dụng mạng nơ-ron RBF*," Journal of Science & Technology - Hanoi University of Industry, Vol. 65, No. 3, pp. 45-53, (2023), doi: 10.57001/huih5804.2023.250 (in Vietnamese).

[6]. P. Mishra *et al.*, "*Model Predictive Control for a 2-DOF Robotic Arm: Dynamics and Control*," 2024 International Conference on Modeling, Simulation & Intelligent Computing (MoSICom), pp. 353-358, (2024), doi: 10.3390/electronics13193903.

[7]. M. Y. Silaa *et al.*, "*Robust Adaptive Sliding Mode Control Using Stochastic Gradient Descent for Robot Arm Manipulator Trajectory Tracking*," Electronics, vol. 13, no. 9, (2024), doi: 10.1109/MoSICom63082.2024.10881967.

TÓM TẮT

Điều khiển trượt thích nghi kết hợp bộ quan sát với hệ số thay đổi theo thời gian sử dụng tổng hợp hệ số Riccati cho tay máy robot

Bài báo trình bày một phương pháp điều khiển trượt thích nghi kết hợp bộ quan sát (AOSMC) sử dụng phương pháp điều chỉnh tham số thích nghi thay đổi theo thời gian và tổng hợp hệ số Riccati (RGS) nhằm điều khiển bám quỹ đạo chính xác cao cho tay máy robot trong điều kiện tồn tại nhiễu loạn và bất định động lực học. Phương pháp điều khiển trượt truyền thống mặc dù có tính bền vững cao nhưng thường gây hiện tượng rung giật lớn và yêu cầu biết chính xác giới hạn của hệ thống. Để khắc phục, cấu trúc AOSMC-RGS được đề xuất kết hợp quan sát nhiễu phi tuyến để ước lượng nhiễu thời gian thực với cơ chế điều chỉnh hệ số khuếch đại dựa trên Riccati theo sai số bám. Phân tích ổn định Lyapunov chặt chẽ chứng minh tính bị chặn và hội tụ của các trạng thái hệ thống. Kết quả mô phỏng trên tay máy robot 2 bậc tự do cho thấy phương pháp AOSMC-RGS giúp cải thiện đáng kể độ chính xác bám, khả năng khử nhiễu và giảm biên độ tín hiệu điều khiển khi so với các bộ điều khiển PID, SMC, ASMC, Fuzzy-ASMC, và RBF-ASMC. Phương pháp đề xuất đạt được thời gian đáp ứng nhanh, độ quá chỉnh nhỏ, giảm tiêu hao năng lượng điều khiển và duy trì độ bền vững, phù hợp triển khai thời gian thực trên các hệ thống robot và cơ điện tử.

Từ khoá: Điều khiển thích nghi; Điều khiển trượt; Phương trình Riccati; Bộ quan sát nhiễu; Tay máy robot; Hệ số học thay đổi theo thời gian.